*Am J Physiol Regul Integr Comp Physiol* 305: R13–R23, 2013.
First published April 17, 2013; doi:10.1152/ajpregu.00221.2012.

# Rescue of dystrophic skeletal muscle by PGC-1α involves restored expression of dystrophin-associated protein complex components and satellite cell signaling

**Katrin Hollinger, Delphine Gardan-Salmon, Connie Santana, Drance Rice, Elizabeth Snella, and Joshua T. Selsby**

*Department of Animal Science, Iowa State University, Ames, Iowa*

Submitted 14 May 2012; accepted in final form 16 April 2013

**Hollinger K, Gardan-Salmon D, Santana C, Rice D, Snella E, Selsby JT.** Rescue of dystrophic skeletal muscle by PGC-1α involves restored expression of dystrophin-associated protein complex components and satellite cell signaling. *Am J Physiol Regul Integr Comp Physiol* 305: R13–R23, 2013. First published April 17, 2013; doi:10.1152/ajpregu.00221.2012.—Duchenne muscular dystrophy is typically diagnosed in the preschool years because of locomotor defects, indicative of muscle damage. Thus, effective therapies must be able to rescue muscle from further decline. We have established that peroxisome proliferator-activated receptor gamma coactivator 1-alpha (*Pgc-1α*) gene transfer will prevent many aspects of dystrophic pathology, likely through upregulation of utrophin and increased oxidative capacity; however, the extent to which it will rescue muscle with disease manifestations has not been determined. Our hypothesis is that gene transfer of *Pgc-1α* into declining muscle will reduce muscle injury compared with control muscle. To test our hypothesis, adeno-associated virus 6 (AAV6) driving expression of *Pgc-1α* was injected into single hind limbs of 3-wk-old *mdx* mice, while the contralateral limb was given a sham injection. At 6 wk of age, treated solei had 37% less muscle injury compared with sham-treated muscles ($P < 0.05$). Resistance to contraction-induced injury was improved 10% ($P < 0.05$), likely driven by the five-fold ($P < 0.05$) increase in utrophin protein expression and increase in dystrophin-associated complex members. Treated muscles were more resistant to fatigue, which was likely caused by the corresponding increase in oxidative markers. *Pgc-1α* overexpressing limbs also exhibited increased expression of genes related to muscle repair and autophagy. These data indicate that the *Pgc-1α* pathway remains a good therapeutic target, as it reduced muscle injury and improved function using a rescue paradigm. Further, these data also indicate that the beneficial effects of *Pgc-1α* gene transfer are more complex than increased utrophin expression and oxidative gene expression.

Duchenne muscular dystrophy; utrophin; gene expression; oxidative; *mdx*

CAUSED BY A MUTATION IN THE dystrophin gene, Duchenne muscular dystrophy (DMD) is the most common fatal X-linked disease. In healthy muscle, the dystrophin protein serves as a functional link between the actin cytoskeleton and the extracellular matrix (ECM) through the dystrophin-associated protein complex (DAPC) (8, 11, 49). Production of an aberrant protein product results in a failure to adequately transmit forces to the ECM and results in damage to the sarcolemma, particularly during lengthening contractions, as well as a number of secondary effects. In addition to a failure to maintain calcium homeostasis, metabolic dysregulation is also associated with the disease (17, 32). The culmination of these cellular events is impaired muscle function (39, 54, 55), as contractile tissue is progressively replaced by adipose and fibrotic tissue (14). DMD is typically diagnosed in preschool-aged boys, after the child shows impaired motor function. Patients are often wheelchair bound by age 12 and succumb to the disease due to respiratory complications or cardiomyopathy in the early 20s (15).

DMD is modeled by the *mdx* mouse, which has a nonsense mutation in exon 23 (7, 56). While the *mdx* mouse is dystrophin-deficient, it generally suffers a far milder phenotype than typical DMD patients. For example, there is generally no fatty infiltration into muscle, the lifespan is only moderately reduced (~20%), and mobility is generally not affected (9). The *mdx* mouse, however, does accurately recapitulate many aspects of the disease for a brief time in the hind limb muscles, while the diaphragm suffers a steady disease progression like that observed in human patients (13, 57). Among the proposed explanations for the mild phenotype of *mdx* mice compared with DMD patients is that *mdx* mice have higher utrophin expression (26). Utrophin is an autosomal dystrophin-related protein that is expressed at the neuromuscular junction (NMJ) in healthy muscle cells (20, 25). Because utrophin has a similar structure to dystrophin ($NH_2$ and COOH termini, spectrin-like repeats, and hinge regions), it has been suggested that utrophin can serve as a functional substitute for dystrophin in dystrophic skeletal muscle (44, 61). Indeed, dystrophin-deficient mice transgenically overexpressing *utrophin* and *utrophin* gene transfer in animal models have shown convincingly that increased utrophin expression will prevent and delay disease onset and rescue already declining muscle (23, 46, 60, 63) from some, but not all dystrophic pathologies (29). Currently, however, a practical means of increasing utrophin expression is lacking for human patients.

Activation of the transcriptional coregulator, peroxisome proliferator-activated receptor gamma coactivator 1-alpha (PGC-1α), promotes the expression of utrophin at the NMJ, as well as more widely throughout the sarcolemma (2, 19). Importantly, PGC-1α also regulates mitochondria biogenesis and promotes the expression of oxidative genes, which may help to offset metabolic dysregulation observed in dystrophic skeletal muscle (17, 27, 32, 65). Moreover, PGC-1α has also been shown to lead to the expression of antioxidants, which may help to reduce free radical injury and maintain muscle function (21, 55, 64). Indeed, dystrophin-deficient mice transgenic for increased *Pgc-1α* and gene delivery of *Pgc-1α* into neonatal *mdx* skeletal muscle have reduced muscle injury and improved muscle function compared with untreated muscle (22, 52).

Address for reprint requests and other correspondence: J. Selsby, 2356 Kildee Hall, Dept. of Animal Science, Iowa State Univ., Ames, IA 50011 USA (e-mail: jselsby@iastate.edu).

These early successes are promising and indicate that *Pgc-1α* overexpression will prevent disease onset. However, as most patients are diagnosed precisely because they have functional impairments, it indicates that they already have advanced disease-related injury sufficient to impact locomotion. Hence, it is important that interventions not only prevent the disease from developing but also prevent continued decline, and potentially even restore muscle function if initiated following the onset of muscle injury. In a recent investigation, *Pgc-1α* gene transfer was performed in 6-wk-old muscle in *mdx* mice (18). Although ultimately effective in improving a number of pathological outcomes, 6-wk-old muscle is well into the regenerative phase of the early necrotic bout; hence, the extent to which PGC-1α alters typical pathology in actively declining muscle remains unknown. The aim of this study is to determine the extent to which *Pgc-1α* gene transfer rescues dystrophic muscle from typical disease-related decline during the initial necrotic bout. This purpose represents an important next step in a line of inquiry advancing PGC-1α pathway activation toward therapeutic application for DMD patients. Our hypothesis is that dystrophic skeletal muscles overexpressing PGC-1α will have less muscle injury and improved function compared with untreated muscles, indicating successful rescue of disease progression.

## METHODS

*Animal treatments.* All animal procedures were approved by the Institutional Animal Care and Use Committee at Iowa State University and were done in accordance with the guiding principles established by the American Physiological Society. To determine the extent to which *Pgc-1α* gene transfer can rescue dystrophic muscle from disease-related decline, 3-wk-old dystrophin-deficient (*mdx*) mice were obtained from our colony. We have found that *mdx* mice from our colony begin to exhibit early signs of muscle injury at approximately this time. Mice were given a 50-μl injection in a single triceps surae containing $1 \times 10^{11}$ genome copies of AAV serotype six driving expression of *Pgc-1α* under the control of a modified chicken β-actin promoter (52). We have previously used a similar technique to achieve infection of the muscles of a single limb, while the contralateral limb remained uninfected (52, 55). The contralateral limb was injected with empty vector. At 6 wk of age, animals were brought to a surgical level of anesthesia with tribromoethanol, the soleus muscles were removed, and the mouse was killed by cervical dislocation. Soleus muscle pairs were randomly assigned to either biochemistry and were snap frozen in liquid nitrogen, or histology, and coated in freezing media and frozen in melting isopentane. In addition, a subset of animals were treated and designated for muscle function measures.

*Histology.* Ten-micrometer frozen sections were cut from soleus muscles and placed on slides. Hematoxylin-and-eosin staining was performed, according to standard techniques. Each soleus muscle was visualized using a Leica microscope at ×100, and multiple pictures were taken, so that the entire soleus was captured, generally using three to five images. Complete soleus muscles were digitally reconstructed using Photoshop, so that the entire muscle cross section was in a single picture file and could be readily analyzed. The reconstructed image was imported into OpenLab, so that areas of immune cell infiltration, hypercontracted cells, and hematoxylin-and-eosin (H&E)-negative cells could be quantified. These areas are expressed as a percentage of the total muscle cross-sectional area. H&E sections were further used to determine central nucleation. Briefly, the total number of muscle fibers and the total number of muscle fibers with centralized nuclei were counted in the reconstructed image using ImageJ. The total number of fibers with a centralized nucleus was made relative to the total number of fibers in the cross section, and the resulting percentage was reported. Counts were made by a blinded technician.

To identify utrophin protein localization and measure expression, slides were probed with antibody for utrophin (Vector VP-U579) directly labeled with Zeon Alexa Fluor 568 (Invitrogen Z25006). Slides were washed in PBS for 10 min and blocked for 15 min with 5% BSA. They were then exposed to labeled primary antibody (1:10) in 1% BSA and incubated for 60 min at room temperature in the dark. Slides were washed three times for 10 min in PBS. Coverslips were mounted using Vectashield with DAPI.

Utrophin expression and localization were visualized in two or three random sections/muscle at ×400. Importantly, all slides were prepared at the same time, and all images were taken using identical exposure conditions on the same microscope in random order. To quantify utrophin expression, images were imported into OpenLab, and the density slice function was used to transform the image into a binary image. In this fashion, pixels are identified as either above or below threshold intensity. Threshold was determined by measuring pixel intensity of intracellular and extracellular areas, where there should be no utrophin expression, as well as utrophin expression at several locations on the sarcolemma in several random sections. Importantly, all images were processed under identical conditions. For sections from control soleus muscles, the replicate with the greatest utrophin expression was used for analysis. Conversely, for the *Pgc-1α*-treated limbs, the corresponding replicate with the lowest utrophin expression was used for analysis. The total area of utrophin expression that exceeded threshold was quantified and is expressed relative to control. As we compared the greatest utrophin expression from control soleus muscles to the lowest utrophin expression from corresponding treated muscles, our measurement of relative utrophin expression is likely conservative.

To determine fiber size distribution, slides were washed and blocked as described above. Overnight, sections were exposed to a primary antibody for laminin (NeoMarkers, RB-082-A) at a dilution of 1:100. Slides were then washed, and secondary antibody applied for 1 h at room temperature. Secondary antibody (goat anti-rabbit-rhodamine conjugated; Millipore, 12-510) was used at a dilution of 1:100. Two random and nonoverlapping images were taken of each section at ×200. Using Image Pro, we measured minimum Feret diameter in each complete cell in these images, and resultant data were pooled for each muscle, resulting in the inclusion of 100–180 fibers/muscle. Average fiber diameter was calculated as was the coefficient of variance (6).

*Muscle function.* Muscle function (tetanic force, a series of eccentric contractions, and fatigue) was measured in the soleus at the Physiological Assessment Core of the Wellstone Muscular Dystrophy Cooperative Center at the University of Pennsylvania, according to standard techniques (3, 4, 36, 39, 52–55). Solei from different animals were used to measure eccentric injury and fatigue resistance, so that one measure would not interfere with the other. Force produced during these measures is normalized to the force produced during the initial contraction. Importantly, technicians performing these measures were blinded to the treatments.

*Biochemistry.* RNA was isolated from soleus muscles using TRIzol following the manufacturer's recommended instructions. Purified RNA was further processed using Qiagen RNeasy spin columns. Using the RT$^2$ first-strand kit (SABiosciences), we synthesized cDNA from 1 μg of purified RNA, following manufacturer's instructions. Subsequently, we performed quantitative PCR (qPCR) to determine *Pgc-1α* expression in treated and control limbs using the 18S ribosomal subunit as a loading control. We also measured expression of the autophagy markers *Lc3* (*Map1lc3a*), *Atg 12*, *Bnip 3*, and *Gabarap 1* in a similar manner. Additionally, cDNA was loaded into SABioscience mouse skeletal muscle: myogenesis and myopathy array (PAMM-099A), and qPCR reactions were run according to the manufacturer's recommendations. The array is a 96-well PCR plate seeded with mouse-specific primer pairs for 84 genes with known

function in skeletal muscle myogensis and myopathy. These primer pairs have been extensively tested for target specificity, according to the manufacturer. Expression of all significantly different genes was increased; however, genes on the array were chosen because of their known involvement in pathological processes. In addition, the array includes controls for genomic contamination, successful reverse transcription, and a control to verify successful quantitative PCR, as well as suggested loading controls. Importantly, expression (CT value) of these loading controls, *Gapdh* and *β-actin*, was altered by our intervention. To determine an appropriate loading control, we compared CT values of all of the genes on the plates and chose *titin* and *Slc2a4* because they had a combination of the highest *P* value and smallest fold change. To provide the most robust loading control, we normalized to the mean expression of these genes. Normalization to the 18S subunit was not possible because primers to the 18S subunit were not part of the array. Delta (Δ) CT values were calculated by subtracting the CT value from the experimental gene from the CT value of the control. These values were used for statistical comparisons. ΔΔCT was calculated by subtraction of the ΔCT of a treated soleus muscle from the ΔCT of the corresponding control soleus muscle. Data are presented as a fold change as calculated by ΔΔCT. Data points more than 2 SDs from the mean were excluded regardless of direction (above or below mean) or group resulting in the exclusion of 17/534 data points.

*Statistics.* Differences in muscle fatigue were evaluated with PROC MIXED in SAS. Remaining data were compared using paired *t*-tests. Significance was set at $P < 0.05$. All data are expressed as means ± SE unless otherwise noted.

## RESULTS

To increase expression of *Pgc-1α*, a virus driving *Pgc-1α* expression was injected into a single hind limb of 3-wk-old *mdx* mice, while the contralateral limb was injected with a null virus containing empty capsid. The 3-wk-old time point was chosen because soleus muscles from *mdx* mice in our colony show early signs of disease-related muscle injury, including immune cell infiltration and degeneration (Fig. 1). Similar findings of early necrotic changes in limb muscles at this time point have been reported by others (7, 33, 45, 47). Three weeks following viral injection, our gene delivery technique successfully increased expression of *Pgc-1α* in soleus muscles from treated limbs compared with soleus muscles from null limbs by ~11-fold (Fig. 2; $P < 0.05$). Soleus muscle mass was similar between groups (*mdx*-Null: 6.2 ± 0.2 mg; *mdx*-PGC-1α: 6.1 ± 0.2 mg; $n = 29$); however, *Pgc-1α* gene transfer caused a reduction in gastrocnemius mass compared with null virus-treated limbs (*mdx*-Null: 102.7 ± 3.6 mg; *mdx*-PGC-1α: 97.0 ± 3.4 mg; $P < 0.05$; $n = 29$). The large sample number reported for this measure is a combination of muscles used for histological, biochemical, and functional analyses.

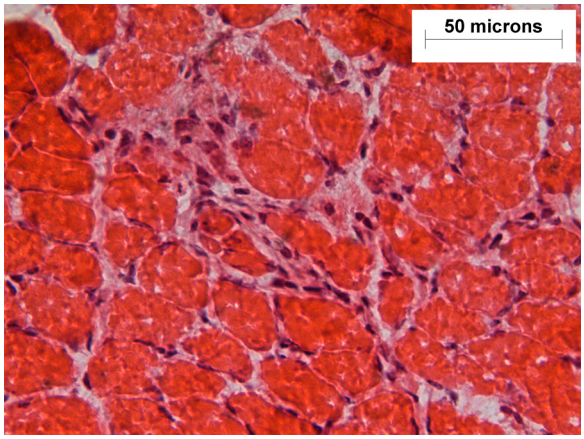


Fig. 1. Disease-related muscle injury in 3-wk-old *mdx* soleus muscle. Following hematoxylin-and-eosin (H&E) staining, early signs of degeneration are apparent at 3 wk of age in dystrophin-deficient soleus muscles. ×400; scale bar = 50 μm.

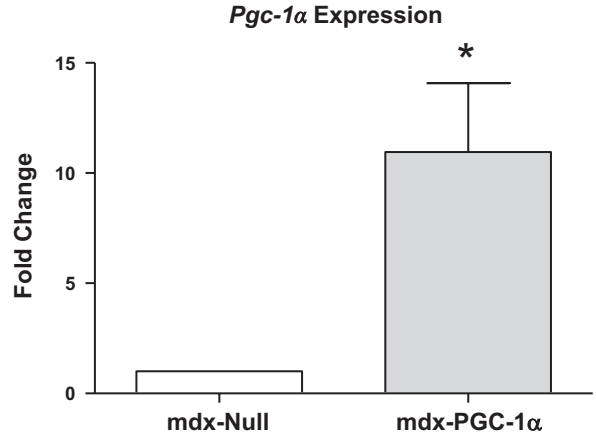


Fig. 2. Gene transfer increases *Pgc-1α* expression. At 3 wk of age, *mdx* mice were injected in a single hind limb with a virus driving expression of *Pgc-1α*, and the contralateral hind limb was given an injection with null virus. At 6 wk of age, soleus muscles were collected and *Pgc-1α* expression measured by qPCR. In treated limbs, *Pgc-1α* expression was 10.96 ± 3.1-fold greater than contralateral limbs. *Significantly different from *mdx*-Null; $n = 8$.

Visual inspection of H&E-stained muscle cross sections revealed disease-related injury to both null-treated and *Pgc-1α*-treated limbs, including foci of necrosis with apparent immune cell infiltration, hypercontracted cells, and H&E-negative staining fibers (Fig. 3). To determine the extent to which PGC-1α altered muscle condition, these areas were quantified. We found that areas of immune cell infiltration were reduced by 31% ($P < 0.05$), areas of hypercontracted cells by 65% ($P < 0.05$), and areas of H&E-negative cells by 43% ($P < 0.05$) in *Pgc-1α*-overexpressing soleus muscles compared with null-virus-treated soleus muscles. In aggregate, this reduced the total area of damaged muscle by 37% ($P < 0.05$). The percentage of cells with centralized nuclei was similar between groups. Fiber area distribution was also similar between groups (Fig. 4), as was the mean minimum Feret diameter and coefficient of variation.

As the total damaged area was decreased in limbs overexpressing *Pgc-1α*, we determined the extent to which *Pgc-1α* gene transfer would rescue muscle function in already declining muscle. Cross-sectional area, tetanic force, and specific tension were similar between groups (Table 1). As there is a rationale to suspect that PGC-1α can lead to utrophin expression and resultant resistance to contraction-induced injury, we measured force production in five eccentric contractions. Solei overexpressing *Pgc-1α* were able to produce ~10% more ($P < 0.05$) force than control solei during each contraction (Fig. 5). To determine the extent to which *Pgc-1α* overexpression rescued *mdx* muscle from fatigue, muscles underwent an endurance challenge. *Pgc-1α* overexpressing solei maintained significantly higher force throughout the protocol ($P < 0.05$) (Fig. 6).

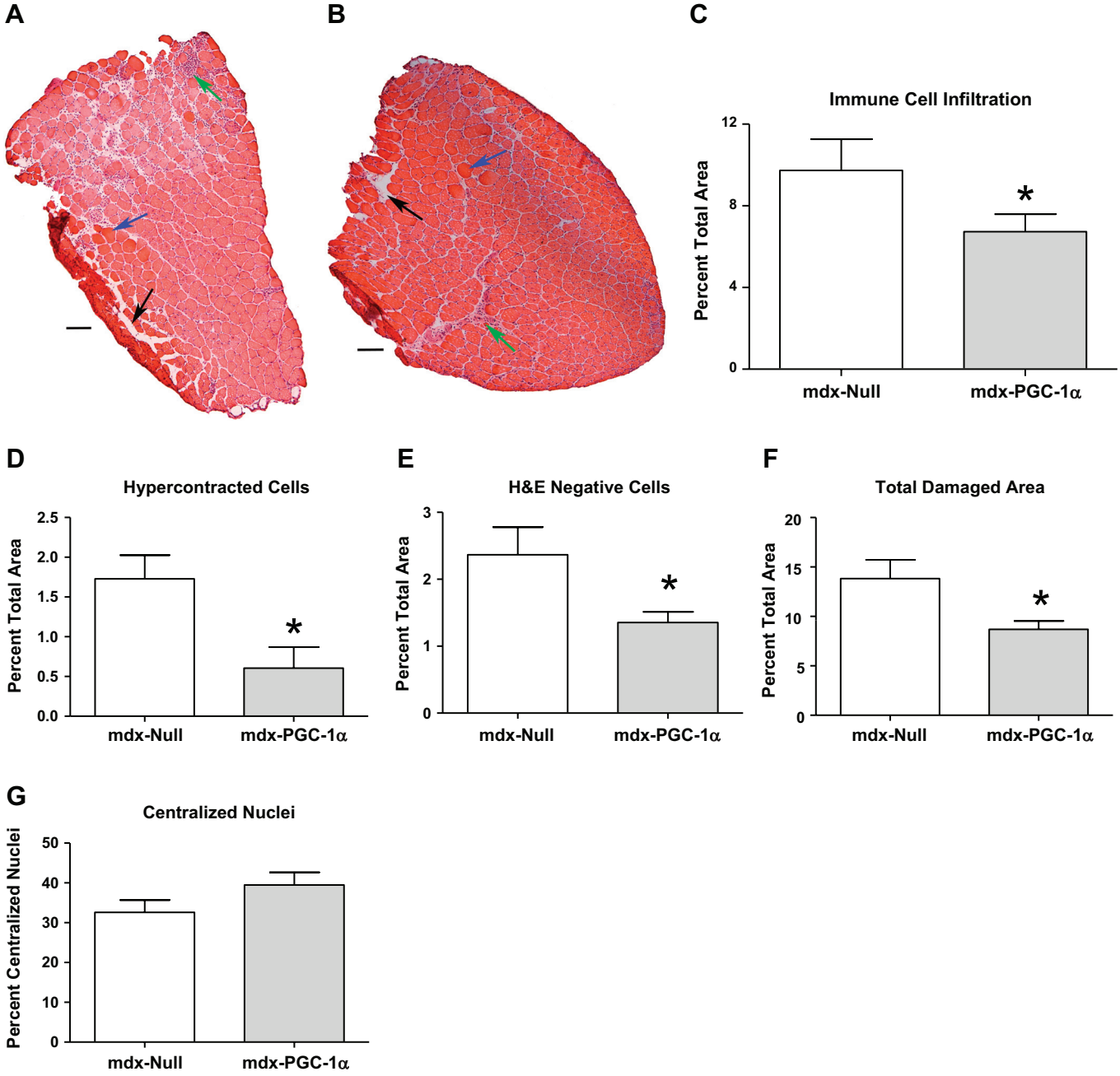


Fig. 3. *Pgc-1α* gene transfer decreases muscle injury. Representative paired soleus muscle cross sections (*mdx*-Null: *A*; *mdx*-PGC-1α: *B*) stained with H&E. Scale bar indicates 100 μm; ×100. Areas of muscle injury were quantified and expressed relative to the total cross-sectional area. Areas of immune cell infiltration (green arrows; *C*), hypercontracted cells (blue arrows; *D*), and H&E-negative cells (black arrows; *E*) were significantly reduced in *Pgc-1α* overexpressing limbs as was the total damaged area (*F*). The percentage of fibers with centralized nuclei was similar between groups (*G*). *Significantly different from *mdx*-Null; $n = 9$.

To better understand the mechanism underlying histological and functional rescue of dystrophic soleus muscles, we measured content and localization of utrophin protein using immunohistochemistry. *Pgc-1α* gene transfer resulted in a nearly five-fold ($P < 0.05$) increase in utrophin expression compared with null-treated soleus muscles (Fig. 7). Importantly, this increase in utrophin was not localized to the neuromuscular junction, as utrophin was found throughout the sarcolemma.

Because PGC-1α is a transcriptional coactivator, it has the potential to alter expression of numerous genes; hence, we performed a PCR array. A PCR array is a 96-well plate preloaded with primers, in this case, for 84 genes involved in myogenesis and myopathy. This array (PAMM-099A, SABiosciences) was selected specifically because it contains primers for genes related to the dystrophin-glycoprotein complex, energy metabolism, and myogenesis, among other processes. Although many of these processes are grounded with sound hypotheses (i.e., increased

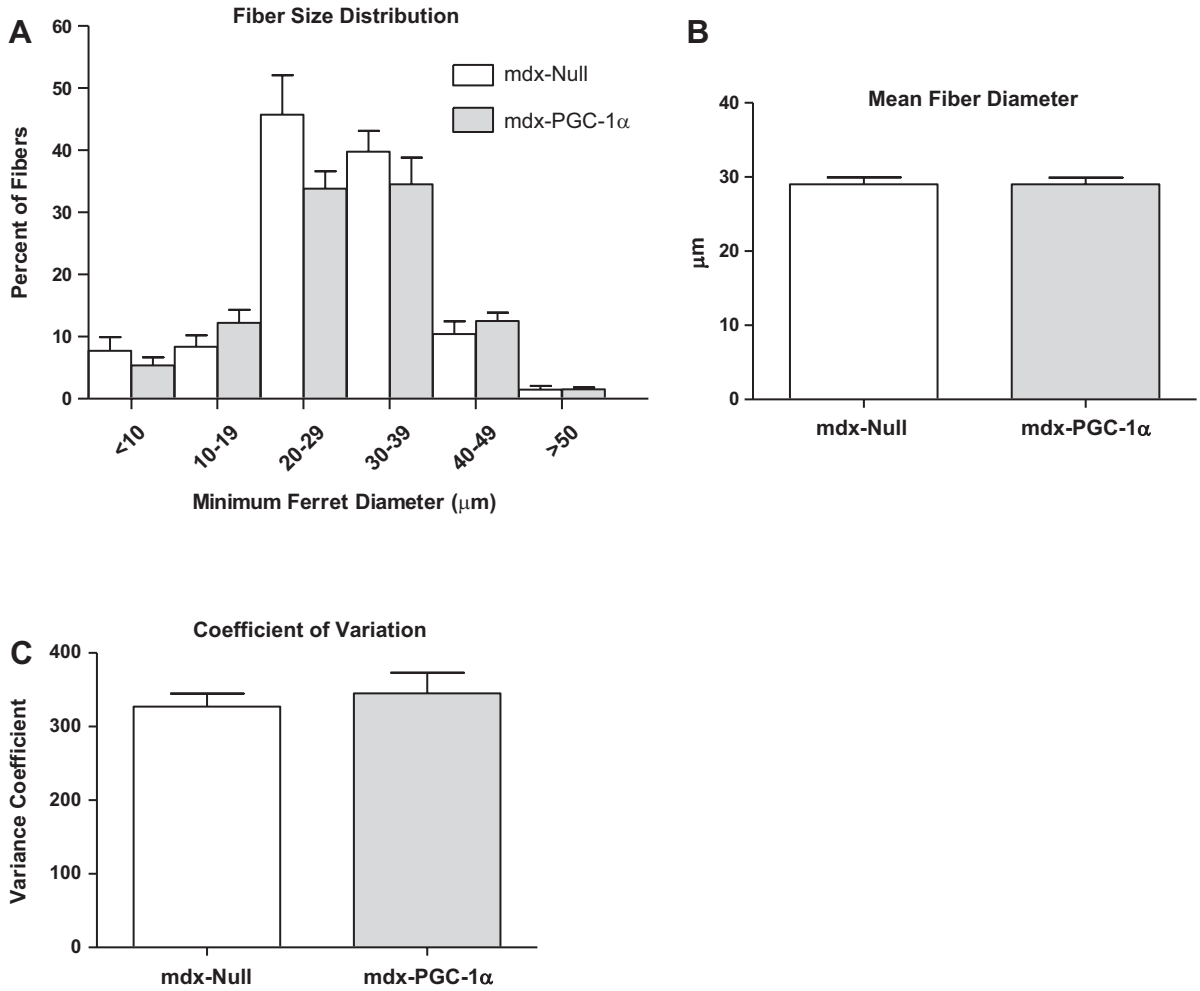


Fig. 4. Fiber size distribution. Fiber size distribution of 6-wk-old soleus muscle did not change following 3 wk of *Pgc-1α* gene transfer. Graphic representation of fiber size distribution (*A*). Mean minimum Ferret diameter (*B*) and the coefficient of variance (*C*) are similar in the *Pgc-1α*-overexpressing and control limb. $n = 8$.

expression of genes related to the DAPC and oxidative metabolism), this approach allowed us to better understand the widespread cellular effects underlying PGC-1α-mediated rescue.

Genes whose products are directly or indirectly associated with dystrophin and the DAPC were increased ~50% (range 33–85%) in soleus muscles overexpressing *Pgc-1α* compared with control muscles (Fig. 8). Expression of several sarcomeric genes was increased, although expression varied widely from 16%, twofold over control soleus muscles (Fig. 8). Expression of metabolic genes was increased 18–85% in soleus muscles from treated limbs compared with soleus muscles from control limbs (Fig. 9), although some metabolic genes failed to reach significance (see Supplemental Table S1). Genes related to satellite cell function were increased 31% to nearly twofold in soleus muscles overexpressing *Pgc-1α* compared with control soleus muscle (Fig. 10). There was a modest increase in genes associated with calcium-mediated protein degradation, as well as the atrogenes *Fbxo 32* (*Atrogin-1*, *MAFbx*) and *Trim 63* (*MuRF 1*) that was countered by an increase in genes associated with protein synthesis in treated limbs compared with control limbs (Fig. 11). Surprisingly, inflammatory signaling was generally increased in treated limbs compared with control limbs. *Tnf* expression was increased 34-fold in treated limbs compared with control limbs and *Il-6* and *Il-1β* were increased by four- and eight-fold, respectively (Fig. 12). Also, proapoptotic *caspase 3* was increased by an approximate 2.6-fold; however, it was well matched with a similar increase in the antiapoptotic *Bcl2* and *αB crystalin* (Fig. 12). Given recent findings using a similar, but distinct, approach (43), we also measured expression of genes related to autophagy. *Pgc-1α* gene transfer caused a 50% and 86% increase in *Lc3* ($P < 0.05$) and *Atg12* ($P < 0.05$), respectively; however, the autophagy genes *Bnip3* and *Gabarap 1* were similar between

Table 1 *Cross-sectional area, tetanic force, or specific tension after Pgc-1α gene transfer*

| | CSA, mm$^2$ | Tetanic Force, mN | Specific Tension, N/cm$^2$ |
|---|---|---|---|
| *mdx*-Null | 0.75 ± 0.04 | 109 ± 8 | 14.6 ± 0.8 |
| *mdx*-PGC-1α | 0.71 ± 0.03 | 104 ± 7 | 14.5 ± 0.6 |

Values are expressed as means ± SE; $n = 11$. *Pgc-1α* gene transfer did not improve cross-sectional area (CSA), tetanic force, or specific tension in solei overexpressing *Pgc-1α* compared to the contralateral control.

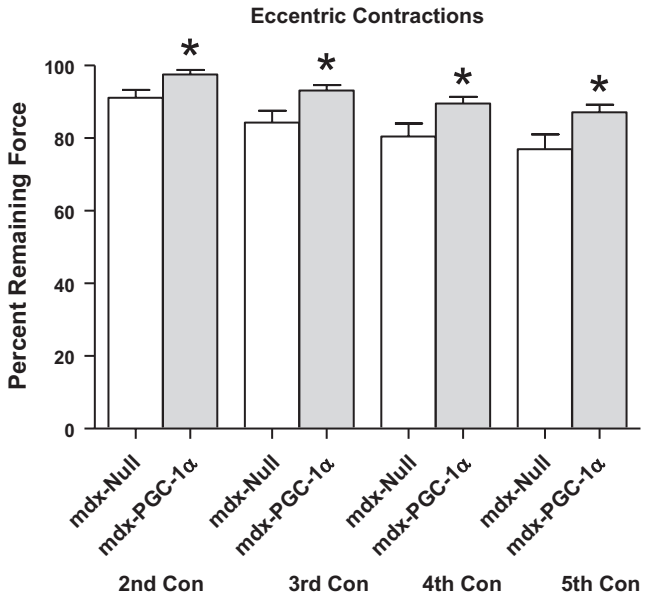


Fig. 5. Force following eccentric contractions. Force decline following eccentric contractions was reduced by *Pgc-1α* gene transfer. Soleus muscles from 6-wk-old *mdx* mice were exposed to five lengthening contractions 3 wk following *Pgc-1α* gene transfer. After all contractions, the force produced by treated soleus muscles was higher compared with control. *Significantly different from *mdx*-null; $n = 5$.

treated and control soleus muscles (Fig. 13). Expression of genes that were similar between groups can be found in Supplemental Table S1.

## DISCUSSION

Duchenne muscular dystrophy is caused by a mutation in the dystrophin gene, giving rise to a nonfunctional protein product. Novel therapies approved for human use have been slow in coming; however, numerous experimental approaches are present in the literature (1, 5, 38, 39, 53–55). Among the most successful is replacing the missing dystrophin protein with utrophin, a dystrophin-related protein (23, 46, 60, 63). Although several strategies for potential use in humans are advancing (24, 35, 62), their approval is not imminent, and drugs may prove ultimately unsuccessful. It is, therefore, critical to continue searching for pathways that can be modulated for therapeutic benefit. One possible solution is to increase expression of the coactivator, PGC-1α, as previous work indicates PGC-1α drives utrophin expression through an N-box domain in the utrophin promoter (2, 22, 37). As well as increased *utrophin* expression, PGC-1α also drives expression of oxidative proteins and antioxidants (21, 28, 64), which may be therapeutic to dystrophic muscle, as metabolic dysregulation has been repeatedly reported (17, 27, 32, 65). Moreover, as PGC-1α is a transcriptional coactivator, there is a likelihood that it will drive expression of additional genes that provide further means of disease mitigation.

An important consideration during therapy development is that DMD patients are generally diagnosed during the preschool years, when they display locomotor deficits, indicating that their muscles have already been damaged by the disease. Hence, interventions must have the potential to rescue declining muscle from continued disease-related muscle injury. We (52), and others (22), have previously established that increased *Pgc-1α* expression prior to muscle injury reduced the severity of disease and preserved muscle function compared with control muscles. Recently, it was shown that *Pgc-1α* gene transfer enhanced recovery from the initial necrotic bout experienced in the *mdx* model (18); however, as the intervention began when muscles would be predicted to be well into the recovery phase, little is known about the capacity of PGC-1α to protect actively declining muscle. In this investigation, our purpose was to extend these observations and determine the extent to which increased *Pgc-1α* expression rescued already declining muscle from continued disease-related muscle injury.

Our injection technique increased *Pgc-1α* expression by ~11-fold compared with control limbs. *Pgc-1α* expression measured by PCR array was similar between groups. One resolution to this discrepancy is that the array targets primers to the 3′ UTR of the transcriptional product, which is lacking in the viral construct. In contrast, our primers are targeted to the middle of the transcriptional product. That endogenous gene expression is similar between limbs indicates that our intervention does not alter expression of endogenous *Pgc-1α*.

We found that gene transfer of *Pgc-1α* into already declining muscle rescued dystrophic muscle from typical disease progression and specifically reduced the areas of immune cell infiltration, hypercontracted cells, and H&E-negative staining fibers. Additionally, *Pgc-1α* overexpression led to resistance to fatigue and injury caused by eccentric contractions. Previously, we found that *Pgc-1α* gene transfer to neonates protected the extensor digitorum longus from eccentric injury, but not the soleus (52). This subtle difference could stem from a more substantial increase of utrophin protein in the current study. Further inconsistencies are found in considering several distinct, but related, interventions: transgenic upregulation of *Pgc-1α*, AICAR (AMPK agonist), and GW501516 (PPARβ/δ agonist). Transgenic *Pgc-1α* overexpression (22) and GW501516 (35) decreased eccentric injury; however, AICAR (31) did not. The increased fatigue resistance found in this study fits well with similar findings after *Pgc-1α* gene transfer in neonates (52).

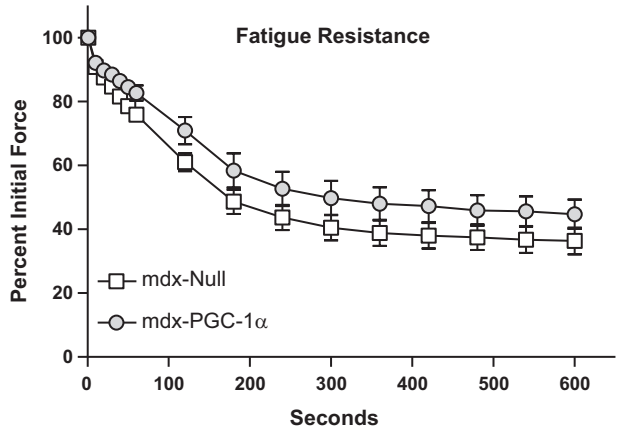


Fig. 6. Fatigue resistance was improved by *Pgc-1α* gene transfer. Soleus muscles from 6-wk-old *mdx* mice were tested for force production during repeated contractions (1/s) 3 wk following *Pgc-1α* gene transfer. The force produced by treated soleus muscles was significantly higher than the force produced by the control soleus muscles throughout the experimental protocol. $n = 6$.

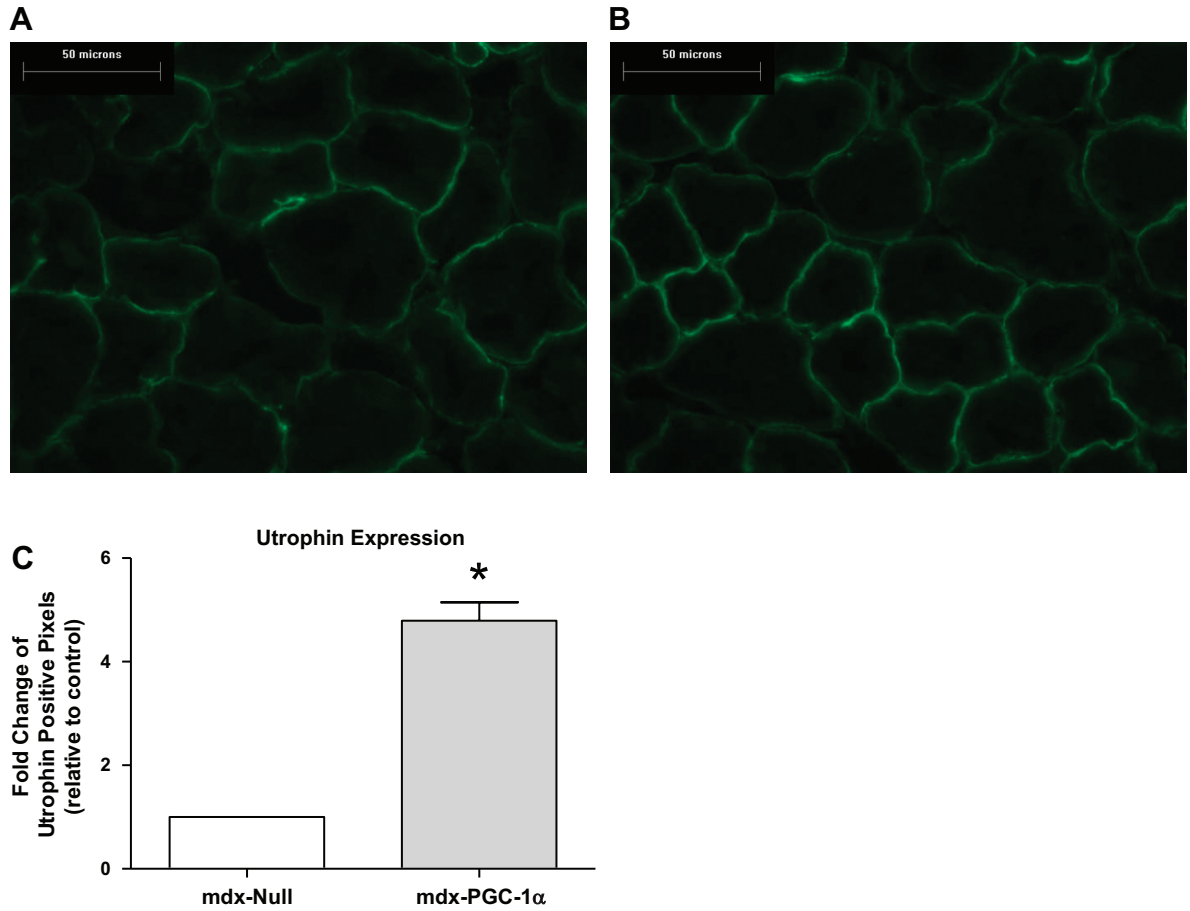


Fig. 7. Utrophin protein expression was increased by *Pgc-1α* gene transfer. Utrophin expression in paired 6-wk-old *mdx* soleus muscles treated with either a null virus (*A*) or a virus driving *Pgc-1α* expression (*B*) after 3 wk of gene transfer. ×400. Scale bar = 50 μm. Within an animal, the replicate with the greatest expression from the control limb was compared with the replicate with the lowest expression from the treated limb (*C*). $n = 3$. *Significantly different from *mdx*-Null.

Consistent with our hypothesis, utrophin gene and protein expression were increased in treated soleus muscles compared with control muscles. Importantly, utrophin protein was located throughout the sarcolemma rather than just focused at the neuromuscular junction. Further, expression of *agrin* was increased in treated soleus muscles compared with control soleus muscles. This potentially provides a secondary means of utrophin expression through an agrin/heregulin pathway (26, 35).

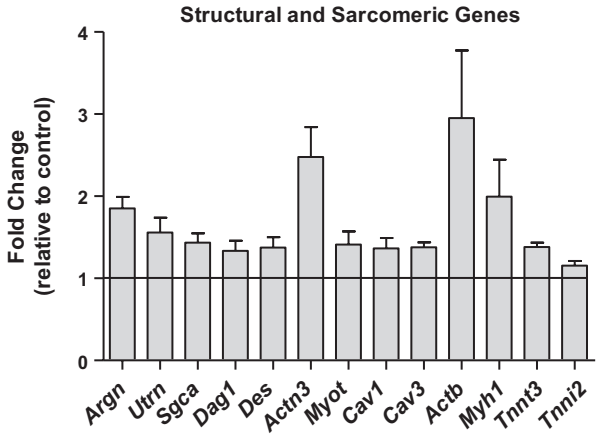


Fig. 8. Fold change of structural and sarcomeric genes altered by *Pgc-1α* gene transfer. Gene expression was measured in 6-wk-old soleus muscles from *mdx* mice 3 wk following *Pgc-1α* gene transfer. $n = 6$. All genes are significantly different compared with control ($P < 0.05$). Fold change relative to *mdx*-Null.

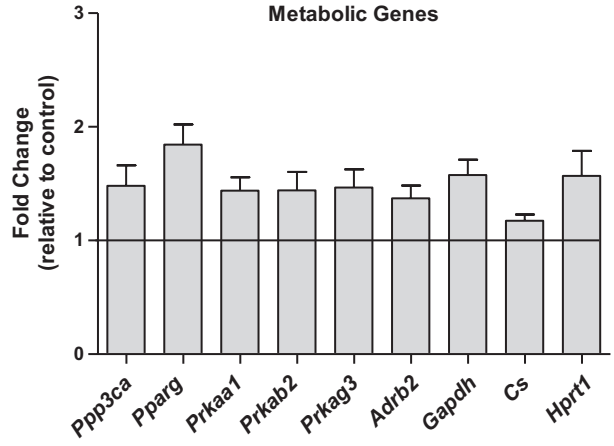


Fig. 9. Fold change of metabolic genes altered by *Pgc-1α* gene transfer. Gene expression was measured in 6-wk-old soleus muscles from *mdx* mice 3 wk following *Pgc-1α* gene transfer. $n = 6$. All genes are significantly different compared with control ($P < 0.05$). Fold change relative to *mdx*-Null.

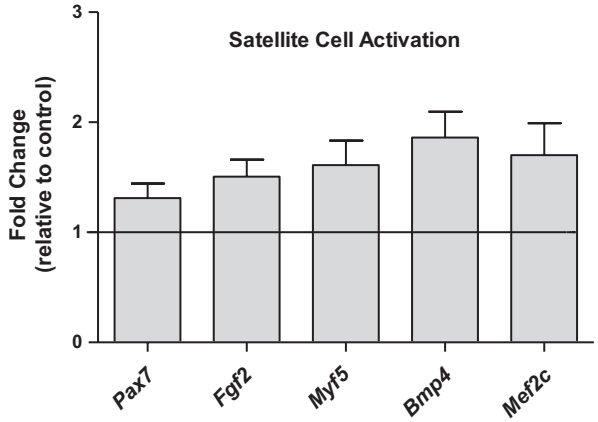


Fig. 10 . Fold change of genes involved in satellite cell activation that changed after *Pgc-1α* gene transfer. Gene expression was measured in 6-wk-old soleus muscles from *mdx* mice 3 wk following *Pgc-1α* gene transfer. $n = 6$. All genes are significantly different compared with control ($P < 0.05$). Fold change relative to *mdx*-Null.

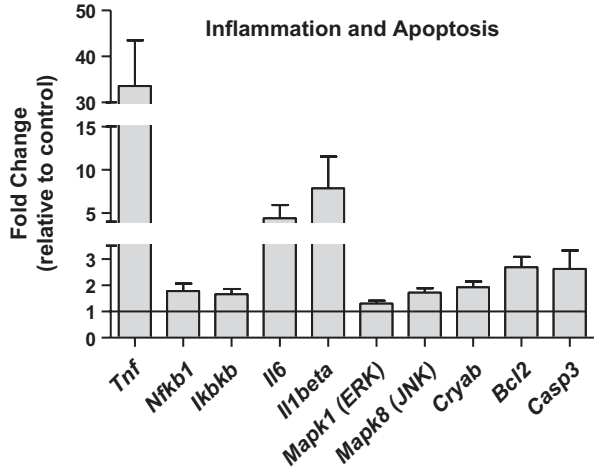


Fig. 12. Fold change of inflammatory and apoptotic genes altered by *Pgc-1α* gene transfer. Gene expression was measured in 6-wk-old soleus muscles from *mdx* mice 3 wk following *Pgc-1α* gene transfer. $n = 6$. All genes are significantly different compared with control ($P < 0.05$). Fold change relative to *mdx*-Null.

Associated with increased utrophin expression was increased expression of sarcoglycan and dystroglycan, genes whose protein products comprise important parts of the DAPC, suggesting that utrophin is functioning as a dystrophin substitute. Of interest, accumulation of dystroglyan, independent of other treatments, has also been shown to decrease disease severity in dystrophic skeletal muscle (34). Improved resistance to damage caused by lengthening contractions indicates that the DAPC components are not only increased but also are functioning. Indeed, numerous other investigations (1, 41) have found that increased utrophin expression leads to increased expression and localization of DAPC components. Increased expression of DAPC components may be directly or indirectly caused by *PGC-1α* gene transfer, but regardless, likely contributes to restoration of sarcolemma stability.

*PGC-1α* gene transfer was expected to lead to robust expression of genes associated with mitochondrial respiration; however, we found this response to be relatively modest. Expression of several oxidative signaling molecules was increased, as expression of three AMPK subunits was increased ~50% and *Pparg* expression was nearly doubled. Consistent with these observations was increased citrate synthase expression, which would allow increased TCA cycle activity. Conversely, *Gapdh* expression was increased, and expression of several oxidative genes was similar between groups (Supplemental Table S1). While the direction of the change in gene expression was generally similar to previous investigations (40, 59), the smaller magnitude of change is likely caused by the shorter duration of this study. Alternatively, it is possible that a rescue paradigm only partially restores metabolic function. Importantly though, the modest increase in oxidative genes translated into increased fatigue resistance in the *Pgc-1α*-expressing solei compared with control muscles.

Contrary to our expectations, the percent of muscle fibers with centralized nuclei, a measure of muscle repair, was similar in treated and nontreated soleus muscles. We anticipated that as PGC-1α pathway activation has been shown to increase

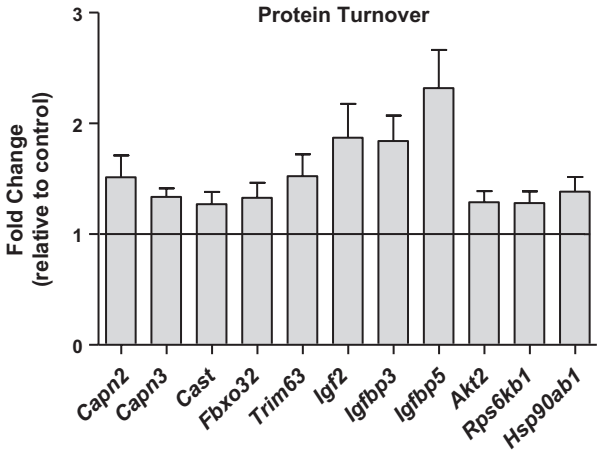


Fig. 11. Fold change of genes involved in protein turnover that changed after *Pgc-1α* gene transfer. Gene expression was measured in 6-wk-old soleus muscles from *mdx* mice 3 wk following *Pgc-1α* gene transfer. $n = 6$. All genes are significantly different compared with control ($P < 0.05$). Fold change relative to *mdx*-Null.

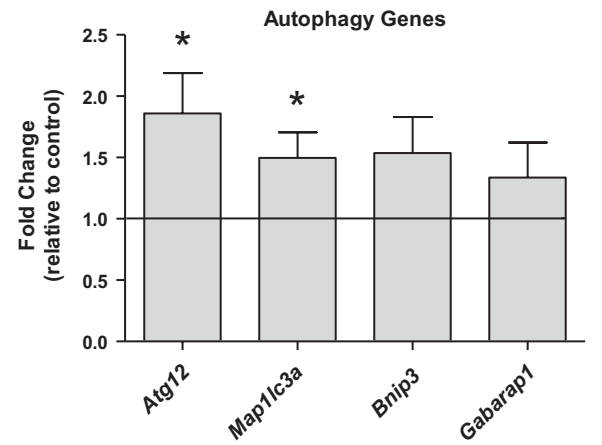


Fig. 13. Fold change of autophagy genes altered by *Pgc-1α* gene transfer. Gene expression was measured in 6-wk-old soleus muscles from *mdx* mice 3 wk following *Pgc-1α* gene transfer. Fold change relative to *mdx*-Null. $n = 6$. *Significantly different from *mdx*-Null.

utrophin expression and reduce muscle injury, the need for repair would be decreased in *Pgc-1α*-overexpressing limbs and be reflected in a lower degree of centralized nuclei. Despite the clear reduction in muscle damage, demonstrated both histologically and functionally, central nucleation was similar between treated and control limbs. Likewise, treatment with GW501516, a PPARβ/δ agonist, which, also led to clear histological and functional benefits, did not result in reduction of central nucleation (35). As both interventions used rescue as a model, as suggested by Miura et al. (35), the central nuclei in this investigation could have resulted from earlier damage and repair. Considering that muscle injury would be predicted to be similar upon treatment, that damage was far less in the *PGC-1α* overexpressing muscles following treatment, and centralized nucleation was similar, an attractive alternative is a PGC-1α-mediated repair process. Indeed, genes leading to increased satellite cell activation (*Pax7*), proliferation (*Pax7*, *Ffg2*, *Bmp4*), self-renewal (*Myf5*), and differentiation (*Mef2c*, *Myf5* in the presence of *MyoD*) were increased in treated soleus muscles compared with control (16, 42, 48, 50, 66, 67). Further, PGC-1α has been shown to interact with and activate *Mef2c* (30). This notion of a PGC-1α-mediated repair process is intriguing, as the proliferative capacity of satellite cells appears to be limited with advanced disease in human patients (58). Hence, a mechanism leading to increased muscle repair is of potential therapeutic importance.

The role of autophagy in dystrophic skeletal muscle is an emerging area of focus, as recent investigations have found that increased (12), not decreased (10), autophagy was associated with decreased disease-related injury. That AICAR led to increased autophagy (43) raised the possibility that *PGC-1α* gene transfer might also perform a similar function. Indeed, expression of *Lc3* and *Atg12*, two key markers associated with autophagy, was induced by PGC-1α, implicating another mechanism by which PGC-1α is decreasing disease-related muscle decline.

While findings generally support a role for increased *PGC-1α* expression as a therapy for dystrophin deficiency, we also measured gene expression contrary to our expectations. For example, despite reduced immune cell infiltration, we found evidence of increased *Tnf* signaling leading to cytokine production and increased expression of *caspase 3* (38). Contrarily, we also found evidence of apoptosis resistance (*Bcl2*, *αB crystalin*) in soleus muscles overexpressing *PGC-1α* compared with contralateral limbs. Further, augmented expression of calpains and atrogenes would suggest increased protein turnover in the *PGC-1α*-treated limbs compared with control limbs and may help to explain decreased muscle mass found in this investigation and others using a similar strategy (31, 52). Conversely, in healthy muscle, transgenic overexpression of *Pgc-1α* led to a reduction in expression of atrogenes after denervation or starvation (51). The roles of inflammatory signaling, apoptosis, and protein turnover are important considerations and will be addressed in future investigations.

In summary, in this investigation, we found that *PGC-1α* gene transfer rescued dystrophic muscle from disease-related decline, suggesting that this strategy could be successful following diagnosis in human patients. We found increased expression of utrophin and DAPC components, increased oxidative gene expression, and autophagy, likely contributing to decreased muscle injury. This was complemented by data pointing toward increased satellite cell activation, indicating an elevated capacity for muscle repair. Thus, PGC-1α leads to multiple mechanisms that synergistically act to decrease disease severity in dystrophin-deficient skeletal muscle. Enthusiasm is dampened, however, as we also measured increased expression of atrogenes, genes involved in apoptotic signaling, and inflammation. Nevertheless, the successful interruption of the disease process through reduced muscle injury and improved muscle function points toward the therapeutic potential of this pathway.

## ACKNOWLEDGMENTS

We thank the Physiological Assessment Core of the Wellstone Muscular Dystrophy Cooperative Center at the University of Pennsylvania and E. R. Barton (supported by Grant U54-AR-052646) for measurement of muscle function and Sandra Rosado and James Koltes for statistical guidance.

## GRANTS

This work was partially supported by a grant from the Center for Integrated Animal Genomics (to J. T. Selsby).

## DISCLOSURES

No conflicts of interest, financial or otherwise, are declared by the authors.

## AUTHOR CONTRIBUTIONS

Author contributions: K.H., D.G.-S., and J.T.S. conception and design of research; K.H., D.G.-S., C.S., D.R., and E.S. performed experiments; K.H., D.G.-S., C.S., D.R., and J.T.S. analyzed data; K.H., D.G.-S., C.S., D.R., and J.T.S. interpreted results of experiments; K.H., D.G.-S., C.S., D.R., and J.T.S. prepared figures; K.H. and J.T.S. drafted manuscript; K.H., E.S., and J.T.S. edited and revised manuscript; K.H., D.G.-S., C.S., D.R., E.S., and J.T.S. approved final version of manuscript.

## REFERENCES

1. **Amenta AR, Yilmaz A, Bogdanovich S, McKechnie BA, Abedi M, Khurana TS, Fallon JR.** Biglycan recruits utrophin to the sarcolemma and counters dystrophic pathology in *mdx* mice. *Proc Natl Acad Sci USA* 108: 762–767, 2011.
2. **Angus LM, Chakkalakal JV, Mejat A, Eibl JK, Belanger G, Megeney LA, Chin ER, Schaeffer L, Michel RN, Jasmin BJ.** Calcineurin-NFAT signaling, together with GABP and peroxisome PGC-1α, drives utrophin gene expression at the neuromuscular junction. *Am J Physiol Cell Physiol* 289: C908–C917, 2005.
3. **Barton ER.** Restoration of gamma-sarcoglycan localization and mechanical signal transduction are independent in murine skeletal muscle. *J Biol Chem* 285: 17263–17270, 2010.
4. **Barton ER, Wang BJ, Brisson BK, Sweeney HL.** Diaphragm displays early and progressive functional deficits in dysferlin-deficient mice. *Muscle Nerve* 42: 22–29, 2010.
5. **Bertoni C.** Clinical approaches in the treatment of Duchenne muscular dystrophy (DMD) using oligonucleotides. *Front Biosci* 13: 517–527, 2008.
6. **Briguet A, Courdier-Fruh I, Foster M, Meier T, Magyar JP.** Histological parameters for the quantitative assessment of muscular dystrophy in the *mdx*-mouse. *Neuromusc Disord* 14: 675–682, 2004.
7. **Bulfield G, Siller WG, Wight PA, Moore KJ.** X chromosome-linked muscular dystrophy (*mdx*) in the mouse. *Proc Natl Acad Sci USA* 81: 1189–1192, 1984.
8. **Byers TJ, Kunkel LM, Watkins SC.** The subcellular distribution of dystrophin in mouse skeletal, cardiac, and smooth muscle. *J Cell Biol* 115: 411–421, 1991.
9. **Chamberlain JS, Metzger J, Reyes M, Townsend D, Faulkner JA.** Dystrophin-deficient *mdx* mice display a reduced life span and are susceptible to spontaneous rhabdomyosarcoma. *FASEB J* 21: 2195–2204, 2007.
10. **Christie KN.** Chymostatin has no apparent beneficial effect on muscular dystrophy in the *mdx* mouse. *J Neurol Sci* 84: 341–346, 1988.
11. **Corrado K, Mills PL, Chamberlain JS.** Deletion analysis of the dystrophin-actin binding domain. *FEBS Lett* 344: 255–260, 1994.

12. **De Palma C, Morisi F, Cheli S, Pambianco S, Cappello V, Vezzoli M, Rovere-Querini P, Moggio M, Ripolone M, Francolini M, Sandri M, Clementi E.** Autophagy as a new therapeutic target in Duchenne muscular dystrophy. *Cell Death Dis* 3: e418, 2012.
13. **Disatnik MH, Dhawan J, Yu Y, Beal MF, Whirl MM, Franco AA, Rando TA.** Evidence of oxidative stress in mdx mouse muscle: studies of the pre-necrotic state. *J Neurol Sci* 161: 77–84, 1998.
14. **Duance VC, Stephens HR, Dunn M, Bailey AJ, Dubowitz V.** A role for collagen in the pathogenesis of muscular dystrophy? *Nature* 284: 470–472, 1980.
15. **Emery AE.** The muscular dystrophies. *Lancet* 359: 687–695, 2002.
16. **Friedrichs M, Wirsdöerfer F, Flohé SB, Schneider S, Wuelling M, Vortkamp A.** BMP signaling balances proliferation and differentiation of muscle satellite cell descendants. *BMC Cell Biol* 12: 26, 2011.
17. **Gardan-Salmon D, Dixon JM, Lonergan SM, Selsby JT.** Proteomic assessment of the acute phase of dystrophin deficiency in *mdx* mice. *Eur J Appl Physiol* 111: 2763–2773, 2011.
18. **Godin R, Daussin F, Matecki S, Li T, Petrof BJ, Burelle Y.** Peroxisome proliferator-activated receptor coactivator 1- gene transfer restores mitochondrial biomass and improves mitochondrial calcium handling in post-necrotic *mdx* mouse skeletal muscle. *J Physiol* 590: 5487–5502, 2012.
19. **Gramolini AO, Belanger G, Thompson JM, Chakkalakal JV, Jasmin BJ.** Increased expression of utrophin in a slow vs. a fast muscle involves posttranscriptional events. *Am J Physiol Cell Physiol* 281: C1300–C1309, 2001.
20. **Gramolini AO, Dennis CL, Tinsley JM, Robertson GS, Cartaud J, Davies KE, Jasmin BJ.** Local transcriptional control of utrophin expression at the neuromuscular synapse. *J Biol Chem* 272: 8117–8120, 1997.
21. **Handschin C, Choi CS, Chin S, Kim S, Kawamori D, Kurpad AJ, Neubauer N, Hu J, Mootha VK, Kim YB, Kulkarni RN, Shulman GI, Spiegelman BM.** Abnormal glucose homeostasis in skeletal muscle-specific PGC-1α knockout mice reveals skeletal muscle-pancreatic β-cell crosstalk. *J Clin Invest* 117: 3463–3474, 2007.
22. **Handschin C, Kobayashi YM, Chin S, Seale P, Campbell KP, Spiegelman BM.** PGC-1α regulates the neuromuscular junction program and ameliorates Duchenne muscular dystrophy. *Genes Dev* 21: 770–783, 2007.
23. **Hirst RC, McCullagh KJ, Davies KE.** Utrophin upregulation in Duchenne muscular dystrophy. *Acta Myol* 24: 209–216, 2005.
24. **Hori YS, Kuno A, Hosoda R, Tanno M, Miura T, Shimamoto K, Horio Y.** Resveratrol ameliorates muscular pathology in the dystrophic *mdx* mouse, a model for Duchenne muscular dystrophy. *J Pharmacol Exp Ther* 338: 784–794, 2011.
25. **Khurana TS, Watkins SC, Chafey P, Chelly J, Tome FM, Fardeau M, Kaplan JC, Kunkel LM.** Immunolocalization and developmental expression of dystrophin-related protein in skeletal muscle. *Neuromuscul Disord* 1: 185–194, 1991.
26. **Law DJ, Allen DL, Tidball JG.** Talin, vinculin and DRP (utrophin) concentrations are increased at *mdx* myotendinous junctions following onset of necrosis. *J Cell Sci* 107: 1477–1483, 1994.
27. **Lehman JJ, Barger PM, Kovacs A, Saffitz JE, Medeiros DM, Kelly DP.** Peroxisome proliferator-activated receptor gamma coactivator-1 promotes cardiac mitochondrial biogenesis. *J Clin Invest* 106: 847–856, 2000.
28. **Leick L, Wojtaszewski JF, Johansen ST, Kiilerich K, Comes G, Hellsten Y, Hidalgo J, Pilegaard H.** PGC-1α is not mandatory for exercise- and training-induced adaptive gene responses in mouse skeletal muscle. *Am J Physiol Endocrinol Metab* 294: E463–E474, 2008.
29. **Li D, Bareja A, Judge L, Yue Y, Lai Y, Fairclough R, Davies KE, Chamberlain JS, Duan D.** Sarcolemmal nNOS anchoring reveals a qualitative difference between dystrophin and utrophin. *J Cell Sci* 123: 2008–2013, 2010.
30. **Lin J, Wu H, Tarr PT, Zhang CY, Wu Z, Boss O, Michael LF, Puigserver P, Isotani E, Olson EN, Lowell BB, Bassel-Duby R, Spiegelman BM.** Transcriptional co-activator PGC-1 alpha drives the formation of slow-twitch muscle fibres. *Nature* 418: 797–801, 2002.
31. **Ljubicic V, Miura P, Burt M, Boudreault L, Khogali S, Lunde JA, Renaud JM, Jasmin BJ.** Chronic AMPK activation evokes the slow, oxidative myogenic program and triggers beneficial adaptations in *mdx* mouse skeletal muscle. *Hum Mol Genet* 20: 3478–3493, 2011.
32. **Lucas-Heron B, Schmitt N, Ollivier B.** Muscular dystrophy: possible role of mitochondrial deficiency in muscle degeneration processes. *J Neurol Sci* 95: 327–334, 1990.
33. **McGeachie JK, Grounds MD, Partridge TA, Morgan JE.** Age-related changes in replication of myogenic cells in *mdx* mice: quantitative autoradiographic studies. *J Neurol Sci* 119: 169–179, 1993.
34. **Miller G, Moore CJ, Terry R, La Riviere T, Mitchell A, Piggott R, Dear TN, Wells DJ, Winder SJ.** Preventing phosphorylation of dystroglycan ameliorates the dystrophic phenotype in *mdx* mouse. *Hum Mol Genet* 21: 4508–4520, 2012.
35. **Miura P, Chakkalakal JV, Boudreault L, Belanger G, Hebert RL, Renaud JM, Jasmin BJ.** Pharmacological activation of PPARβ/δ stimulates utrophin A expression in skeletal muscle fibers and restores sarcolemmal integrity in mature *mdx* mice. *Hum Mol Genet* 18: 4640–4649, 2009.
36. **Moorwood C, Liu M, Tian Z, Barton ER.** Isometric and eccentric force generation assessment of skeletal muscles isolated from murine models of muscular dystrophies. *J Vis Exp* e50036, 2013.
37. **Mootha VK, Handschin C, Arlow D, Xie X, St Pierre J, Sihag S, Yang W, Altshuler D, Puigserver P, Patterson N, Willy PJ, Schulman IG, Heyman RA, Lander ES, Spiegelman BM.** Erralpha and Gabpa/b specify PGC-1α-dependent oxidative phosphorylation gene expression that is altered in diabetic muscle. *Proc Natl Acad Sci USA* 101: 6570–6575, 2004.
38. **Morine KJ, Bish LT, Selsby JT, Gazzara JA, Pendrak K, Sleeper MM, Barton ER, Lee SJ, Sweeney HL.** Activin IIB receptor blockade attenuates dystrophic pathology in a mouse model of Duchenne muscular dystrophy. *Muscle Nerve* 42: 722–730, 2010.
39. **Morris CA, Selsby JT, Morris LD, Pendrak K, Sweeney HL.** Bowman-Birk inhibitor attenuates dystrophic pathology in *mdx* mice. *J Appl Physiol* 109: 1492–1499, 2010.
40. **Nikolic N, Rhedin M, Rustan AC, Storlien L, Thoresen GH, Stromstedt M.** Overexpression of PGC-1α increases fatty acid oxidative capacity of human skeletal muscle cells. *Biochem Res Int* 2012: 714074, 2012.
41. **Odom GL, Gregorevic P, Allen JM, Finn E, Chamberlain JS.** Microutrophin delivery through rAAV6 increases lifespan and improves muscle function in dystrophic dystrophin/utrophin-deficient mice. *Mol Ther* 16: 1539–1545, 2008.
42. **Ono Y, Calhabeu F, Morgan JE, Katagiri T, Amthor H, Zammit PS.** BMP signalling permits population expansion by preventing premature myogenic differentiation in muscle satellite cells. *Cell Death Differ* 18: 222–234, 2011.
43. **Pauly M, Daussin F, Burelle Y, Li T, Godin R, Fauconnier J, Koechlin-Ramonatxo C, Hugon G, Lacampagne A, Coisy-Quivy M, Liang F, Hussain S, Matecki S, Petrof BJ.** AMPK activation stimulates autophagy and ameliorates muscular dystrophy in the *mdx* mouse diaphragm. *Am J Pathol* 181: 583–592, 2012.
44. **Pearce M, Blake DJ, Tinsley JM, Byth BC, Campbell L, Monaco AP, Davies KE.** The utrophin and dystrophin genes share similarities in genomic structure. *Hum Mol Genet* 2: 1765–1772, 1993.
45. **Radley HG, Grounds MD.** Cromolyn administration (to block mast cell degranulation) reduces necrosis of dystrophic muscle in mdx mice. *Neurobiol Dis* 23: 387–397, 2006.
46. **Rafael JA, Tinsley JM, Potter AC, Deconinck AE, Davies KE.** Skeletal muscle-specific expression of a utrophin transgene rescues utrophin-dystrophin deficient mice. *Nat Genet* 19: 79–82, 1998.
47. **Rayavarapu S, Coley W, Cakir E, Jahnke V, Takeda S, Aoki Y, Gordish-Dressman H, Jaiswal JK, Hoffman EP, Brown KJ, Hathout Y, Nagaraju K.** Identification of disease-specific pathways using in vivo SILAC proteomics in dystrophin-deficient *mdx* mouse. *Mol Cell Proteomics* 12: 1061–1073, 2013.
48. **Ridgeway AG, Wilton S, Skerjanc IS.** Myocyte enhancer factor 2C and myogenin up-regulate each other's expression and induce the development of skeletal muscle in P19 cells. *J Biol Chem* 275: 41–46, 2000.
49. **Rybakova IN, Amann KJ, Ervasti JM.** A new model for the interaction of dystrophin with F-actin. *J Cell Biol* 135: 661–672, 1996.
50. **Sabourin LA, Girgis-Gabardo A, Seale P, Asakura A, Rudnicki MA.** Reduced differentiation potential of primary MyoD−/− myogenic cells derived from adult skeletal muscle. *J Cell Biol* 144: 631–643, 1999.
51. **Sandri M, Lin J, Handschin C, Yang W, Arany ZP, Lecker SH, Goldberg AL, Spiegelman BM.** PGC-1 alpha a protects skeletal muscle from atrophy by suppressing Fox03 action and atrophy-specific gene transcription. *Proc Natl Acad Sci USA* 103: 16260–16265, 2006.
52. **Selsby J, Morine K, Pendrak K, Barton E, Sweeney HL.** Rescue of dystrophic skeletal muscle by PGC-1a involves a fast to slow fiber type shift in the *mdx* mouse. *PLoS One* 7: e30063, 2012.

53. **Selsby J, Morris C, Morris L, Sweeney L.** A proteasome inhibitor fails to attenuate dystrophic pathology in *mdx* mice. *PLoS Currents* 4: e4f84a944d8930, 2012.
54. **Selsby J, Pendrak K, Zadel M, Tian Z, Pham J, Carver T, Acosta P, Barton E, Sweeney HL.** Leupeptin-based inhibitors do not improve the mdx phenotype. *Am J Physiol Regul Integr Comp Physiol* 299: R1192–R1201, 2010.
55. **Selsby JT.** Increased catalase expression improves muscle function in *mdx* mice. *Exp Physiol* 96: 194–202, 2011.
56. **Sicinski P, Geng Y, Ryder-Cook AS, Barnard EA, Darlison MG, Barnard PJ.** The molecular basis of muscular dystrophy in the mdx mouse: a point mutation. *Science* 244: 1578–1580, 1989.
57. **Stedman HH, Sweeney HL, Shrager JB, Maguire HC, Panettieri RA, Petrof B, Narusawa M, Leferovich JM, Sladky JT, Kelly AM.** The *mdx* mouse diaphragm reproduces the degenerative changes of Duchenne muscular dystrophy. *Nature* 352: 536–539, 1991.
58. **Sterrenburg E, van der Wees CG, White SJ, Turk R, de Menezes RX, van Ommen GJ, den Dunnen JT, 't Hoen PA.** Gene expression profiling highlights defective myogenesis in DMD patients and a possible role for bone morphogenetic protein 4. *Neurobiol Dis* 23: 228–236, 2006.
59. **Summermatter S, Baum O, Santos G, Hoppeler H, Handschin C.** Peroxisome proliferator-activated receptor γ coactivator 1α (PGC-1α) promotes skeletal muscle lipid refueling in vivo by activating de novo lipogenesis and the pentose phosphate pathway. *J Biol Chem* 285: 32793–32800, 2010.
60. **Tinsley J, Deconinck N, Fisher R, Kahn D, Phelps S, Gillis JM, Davies K.** Expression of full-length utrophin prevents muscular dystrophy in *mdx* mice. *Nat Med* 4: 1441–1444, 1998.
61. **Tinsley JM, Blake DJ, Roche A, Fairbrother U, Riss J, Byth BC, Knight AE, Kendrick-Jones J, Suthers GK, Love DR, Edwards YH, Davies, KE.** Primary structure of dystrophin-related protein. *Nature* 360: 591–593, 1992.
62. **Tinsley JM, Fairclough RJ, Storer R, Wilkes FJ, Potter AC, Squire SE, Powell DS, Cozzoli A, Capogrosso RF, Lambert A, Wilson FX, Wren SP, De Luca A, Davies KE.** Daily treatment with SMTC1100, a novel small molecule utrophin upregulator, dramatically reduces the dystrophic symptoms in the *mdx* mouse. *PLos One* 6: e19189, 2011.
63. **Tinsley JM, Potter AC, Phelps SR, Fisher R, Trickett JI, Davies KE.** Amelioration of the dystrophic phenotype of *mdx* mice using a truncated utrophin transgene. *Nature* 384: 349–353, 1996.
64. **Wenz T, Rossi SG, Rotundo RL, Spiegelman BM, Moraes CT.** Increased muscle PGC-1α expression protects from sarcopenia and metabolic disease during aging. *Proc Natl Acad Sci USA* 106: 20405–20410, 2009.
65. **Wu Z, Puigserver P, Andersson U, Zhang C, Adelmant G, Mootha V, Troy A, Cinti S, Lowell B, Scarpulla RC, Spiegelman BM.** Mechanisms controlling mitochondrial biogenesis and respiration through the thermogenic coactivator PGC-1. *Cell* 98: 115–124, 1999.
66. **Yablonka-Reuveni Z, Seger R, Rivera AJ.** Fibroblast growth factor promotes recruitment of skeletal muscle satellite cells in young and old rats. *J Histochem Cytochem* 47: 23–42, 1999.
67. **Zammit PS, Relaix F, Nagata Y, Ruiz AP, Collins CA, Partridge TA, Beauchamp JR.** Pax7 and myogenic progression in skeletal muscle satellite cells. *J Cell Sci* 119: 1824–1832, 2006.